Inorganic Chemistry
Cite This: Inorg. Chem. XXXX, XXX, XXX−XXX
Article
pubs.acs.org/IC

Cyclopentadienyl−Ru(II)−Pyridylamine Complexes: Synthesis, X-ray Structure, and Application in Catalytic Transformation of Bio-Derived Furans to Levulinic Acid and Diketones in Water

Ambikesh D. Dwivedi, Vinod K. Sahu, Shaikh M. Mobin, and Sanjay K. Singh*

Discipline of Chemistry, School of Basic Sciences, Indian Institute of Technology Indore, Simrol 453552, Indore, India

Supporting Information

ABSTRACT: A series of cationic half-sandwich cyclopentadienyl−ruthenium(II)−pyridylamine complexes, $[(\eta^5\text{-}C_5H_5)Ru(\kappa^2\text{-}L)(PPh_3)]^+$ (L = N_{amine}-substituted pyridylamine ligands) ([**Ru**]-**1**−[**Ru**]-**6**), along with the analogous cyclopentadienyl−ruthenium(II)−*N*-isopropylpyridylimine complex $[(\eta^5\text{-}C_5H_5)Ru(\kappa^2\text{-}L)(PPh_3)]^+$ (L = *N*-isopropylpyridylimine) ([**Ru**]-**7**), have been synthesized in good yields. Structural identities of all the complexes have been authenticated by ^1H, ^{13}C, and ^{31}P NMR, mass spectrometry, and X-ray crystallography. The synthesized complexes exhibited high catalytic activity for the transformation of the bio-derived furans, 2-furfural (furfural), 5-methyl-2-furfural (5-MF), and 5-hydroxymethyl-2-furfural (5-HMF) to levulinic acid (LA) and the diketones, 3-hydroxyhexane-2,5-dione (3-HHD), 1-hydroxyhexane-2,5-dione (1-HHD), and hexane-2,5-dione (HD) in water. Efficient transformation of furfural to LA over a range of η^5-Cp−Ru−pyridylamine complexes is substantially affected by the N_{amine}-substituents, where a η^5-Cp−Ru−*N*-propylpyridylamine complex ([**Ru**]-**2**) exhibited higher catalytic activity in comparison to other η^5-Cp−Ru−pyridylamine and η^5-Cp−Ru−pyridylimine complexes. The relative catalytic activity of the studied complexes demonstrated a substantial structure−activity relationship which is governed by the basicity of N_{amine}, steric hindrance at N_{amine}, and the hemilabile nature of the coordinated pyridylamine ligands.

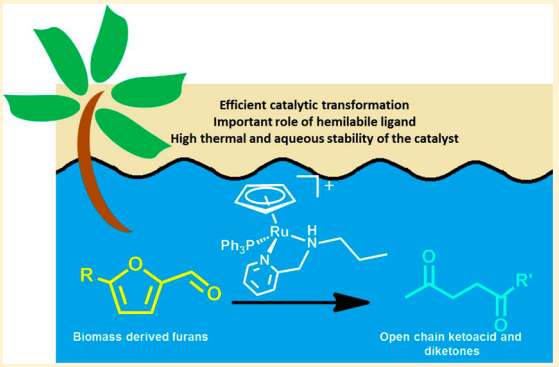

INTRODUCTION

Tremendous interest toward the development of a wide range of stable cyclopentadienyl−Ru(II) (η^5-Cp−Ru) complexes has been observed over the past five decades.[1,2] Consequently, due to the unique structural properties, stability, and chemical reactivity of the η^5-Cp−Ru(II) complexes, these complexes find application in various fields (Scheme 1), including small-molecule activation, transfer hydrogenation, and biology.[3−19] In the particular context of catalysis, one of the prominent η^5-Cp−Ru(II)-based transfer hydrogenation catalysts is Shvo's catalyst, which demonstrated the involvement of both the metal and the ligand to control the selectivity.[10,11] Nikonov's group also demonstrated the application of $[(\eta^5\text{-}C_5H_5)Ru(^iPr_3P)(NCCH_3)_2]$ in the transfer hydrogenation of ketones, nitriles, esters, and N-heterocycles.[12,13] Studies demonstrated the formation of $(\eta^5\text{-}C_5H_5)Ru-H$ (ruthenium hydride) as an important intermediate species, which facilitated the transfer hydrogenation of these unsaturated groups.[14−16] Moreover, mechanistic studies by NMR also revealed the presence of the trihydride species $[(\eta^5\text{-}C_5H_5)Ru(NHC)(H)_3]$ (NHC is a carbene ligand) as the catalyst resting stage for the transfer hydrogenation reaction.[16] Weissensteiner et al. also demonstrated the catalytic reactivity of the η^5-Cp−Ru(II) aminophosphine (PN) complexes $[(\eta^5\text{-}C_5H_5)Ru(\kappa^2\text{-}PN)CH_3CN]^+$ and $[(\eta^5\text{-}C_5H_5)Ru(\kappa^2\text{-}PN)Br]$ for the transfer hydrogenation of a wide range of ketones to secondary alcohols.[17] They proposed that the observed high catalytic activity of these η^5-Cp−Ru(II) aminophosphine complexes is due to the reversible Ru−N bond cleavage of a η^5-Cp−Ru(II)-coordinated aminophosphine ligand (Scheme 1). Similarly, Pandey et al. explored η^5-Cp−Ru(II) complexes containing pyridylphosphine ligands, such as $[(\eta^5\text{-}C_5H_5)Ru(PyPPh_2)(PPh_3)Cl]$, for the transfer hydrogenation of aldehydes to alcohols in the presence of HCOOH/NaOH.[18] Notably, these aminophosphine or pyridylphosphine ligands may act as hemilabile ligands due to their reversible $\kappa^2-\kappa^1-\kappa^2$ coordination behavior to the η^5-Cp−Ru(II) center. These results implied that η^5-Cp−Ru(II) complexes represent an important class of catalyst for transfer hydrogenation reaction, but so far the application of η^5-Cp−Ru(II) complexes in catalytic biomass transformations remains unexplored.[11]

Catalytic transformation of biomass-derived furans and their derivatives to open ring components, such as levulinic acid (LA) and diketones, which are considered as important platform precursors for the production of various fine chemicals and fuel components, have been extensively explored using various heterogeneous catalysts.[19−22] These transformations were mostly carried out in the presence of catalysts based on Pt-, Pd-, Rh-,

Received: March 1, 2018

DOI: 10.1021/acs.inorgchem.8b00536
Inorg. Chem. XXXX, XXX, XXX−XXX

Scheme 1. Literature Reports on Cyclopentadienyl−Ruthenium-Based Complexes

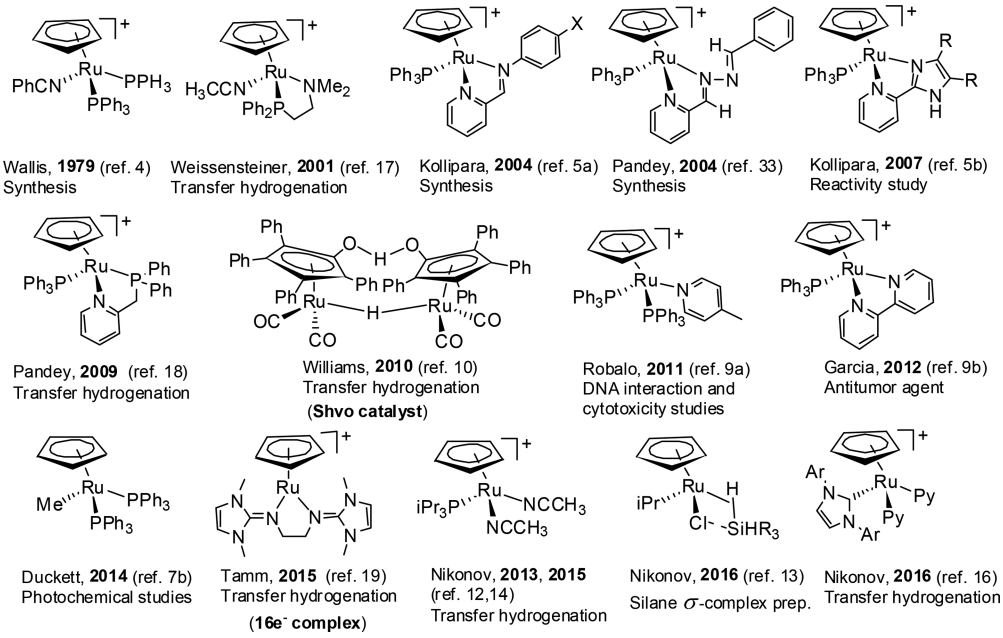

Ru-, and Au-metal-based nanoparticles or in the presence of strong acid (H_3PO_4, HCl, H_2SO_4), high temperature (120−170 °C), and high H_2 pressure (50−100 bar).[20−22] For instance, Montech et al. reported the transformation of 5-hydroxymethylfurfural (5-HMF) to 1-HHD (1-hydroxyhexane-2,5-dione) over Pt/C catalyst in oxalic acid at 140 °C and 30 bar of H_2.[20] Similarly, a 5-HMF to 1-HHD transformation was also reported over Pd/C with Amberlyst-15 under 50 bar of H_2.[21] Analogously, transformation of furans to LA was achieved over Pd/Al_2O_3 with Amberlyst-70 at 165 °C and 70 bar of H_2, as reported by Li et al.[22]

In comparison to the extensive exploration of heterogeneous catalytic systems, catalysts based on transition-metal complexes have been less explored for such biomass transformations. In this direction, Zhang et al. reported $[(\eta^5\text{-Cp}^*)\text{Ir}(\kappa^2\text{-bpy})\text{Cl}]^+$ (where "bpy" is bipyridine) complexes for the catalytic hydrogenolytic transformation of 5-HMF to 1-HHD in water using H_2 gas (10 bar) at 120 °C.[23,24] Later, Fu et al. also investigated the catalytic transformation of 5-HMF to 1-HHD using formic acid/formate buffer solution at 130 °C and 30 bar of H_2, over η^5-Cp*−Ir complexes having hydroxyl-substituted bipyridine ligands, where the hydroxyl substituents exerted a promotional effect to enhance the catalytic performance.[25,26] Moreover, the transformation of LA to γ-valerolactone (GVL) was also explored with Shvo's catalyst.[11] The results implied that a ruthenium−hydride species, $[\{\eta^5\text{-}(C_4\text{-}2,5\text{-}(Ph)_2\text{-}3,4\text{-}(Ar)_2)\}\text{Ru}(CO)_2\text{H}]$, played a crucial role in facilitating the selective transfer hydrogenation of LA to 4-hydroxyvaleric acid (4-HVA) in the presence of formic acid, which was followed by the dehydration of 4-HVA to GVL at 100 °C.[11] In the recent past, we also explored several half-sandwich η^6-arene−Ru(II) complexes having nitrogen donor ligands, $[(\eta^6\text{-arene})\text{Ru}(\kappa^2\text{-L})\text{Cl}]^+$ (L = ethylenediamine or 8-aminoquinoline), for the catalytic transformation of biomass-derived furans such as furfural and 5-HMF to LA and diketones (1-HHD and 3-hydroxyhexane-2,5-dione (3-HHD)) using formic acid.[27,28] Our findings revealed that the presence of −NH groups in these complexes and the presence of a labile coordinating chloro ligand facilitated efficient transfer hydrogenation of furfural to furfuryl alcohol with the aid of formic acid. Subsequently, upon the formation of furfuryl alcohol, H^+-assisted ring opening of furfuryl alcohol led to the formation of LA and diketones. Notably, using formic acid is advantageous, as it can act as an efficient hydrogenating source as well as controls the pH of the catalytic reaction and hence the selectivity of the product. Moreover, η^6-arene−ruthenium complexes usually underwent decomposition to ruthenium metal at higher temperature (>120 °C) and lost their catalytic activity.[29,30] On the other hand, the ruthenium−cyclopentadienyl-based complexes displayed high stability in water and acid at a higher temperature in comparison to η^6-arene−ruthenium complexes.[31,32] It has been hypothesized that the anionic cyclopentadienyl ligand bonded strongly with the Ru^{2+} center, in comparison to the weakly bonded neutral η^6-arene ligand.[31,32] Moreover, it has also been suggested that, due to the anionic cyclopentadienyl ligand, the metal center may have a higher electron density and it may therefore substantially influence the catalytic activity of the resulting η^5-Cp−Ru(II) complexes, in comparison to the η^6-arene ligand.

Herein, we report a series of half-sandwich η^5-Cp−Ru(II) complexes containing N_{amine}-substituted pyridylamine ligands, and the molecular structure of all these complexes have been authenticated by X-ray crystallography. These complexes have been employed for the catalytic ring-opening transformation of the bio-derived furfural, 5-HMF, and other related furans to LA and diketones in water at 120 °C with the aid of formic acid. Our findings evidenced that the presence of −NH bonds, suitably balanced basicity, bulkiness at N_{amine}, and the flexible nature of the pyridylamine ligands significantly influence the outcome of the studied catalytic transformation. Moreover, efficient direct transformation of fructose to diketone and a scaled up (gram-scale) transformation of furfural to levulinic acid are also achieved over the high-performing η^5-Cp−Ru(II)−pyridylamine catalyst.

RESULTS AND DISCUSSION

Synthesis and Characterization of Cyclopentadienyl−Ruthenium(II) Complexes. At the outset, the η^5-Cp−Ru(II) precursor $[(\eta^5\text{-}C_5H_5)\text{RuCl}(\text{PPh}_3)_2]$ was treated with the

DOI: 10.1021/acs.inorgchem.8b00536
Inorg. Chem. XXXX, XXX, XXX−XXX

Scheme 2. Synthesis of η^5-Cp−Ru(II) Complexes Containing Pyridylamine-Based ([Ru]-1−[Ru]-6) and Pyridylimine-Based ([Ru]-7) Ligands

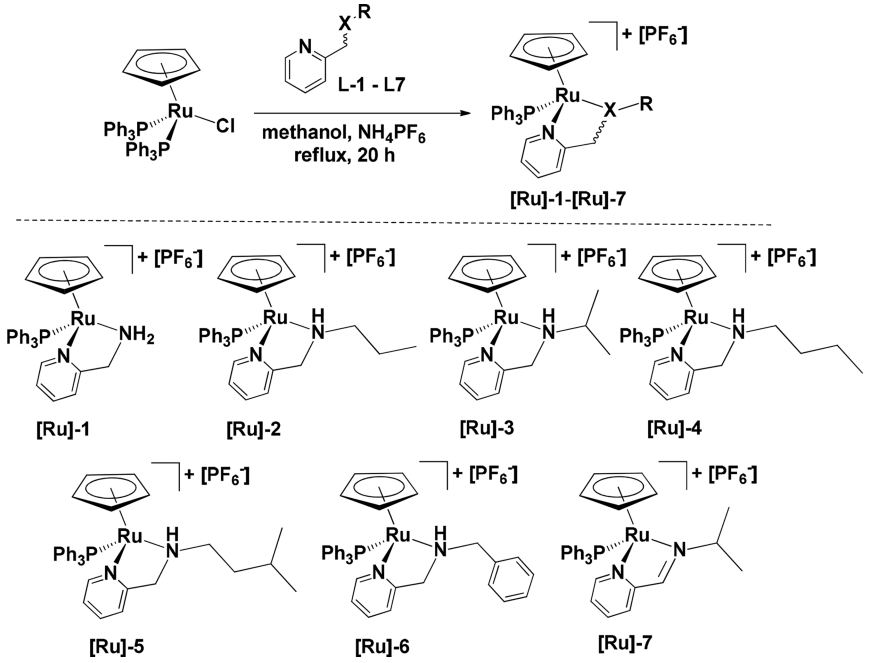

N_{amine}-substituted pyridyamine ligands **L1**−**L6**, 2-(aminomethyl)-pyridine (**L1**), *N*-(pyridin-2-ylmethyl)propan-1-amine (**L2**), *N*-(pyridin-2-ylmethyl)propan-2-amine (**L3**), *N*-(pyridin-2-ylmethyl)butan-1-amine (**L4**), 3-methyl-*N*-(pyridin-2-ylmethyl)butan-1-amine (**L5**), and *N*-benzyl-1-(pyridin-2-yl)-methanamine (**L6**), in methanol under reflux conditions, which afforded yellow to orange cationic mononuclear piano-stool η^5-Cp−Ru(II) complexes [**Ru**]-**1**−[**Ru**]-**6** in good yields (Scheme 2). With the dissociation of a PPh_3 and chloro ligand, the obtained complexes [**Ru**]-**1**−[**Ru**]-**6** have the general formula $[(\eta^5\text{-}C_5H_5)Ru(\kappa^2\text{-L})PPh_3]^+$, where L = **L1** ([**Ru**]-**1**), **L2** ([**Ru**]-**2**), **L3** ([**Ru**]-**3**), **L4** ([**Ru**]-**4**), **L5** ([**Ru**]-**5**), **L6** ([**Ru**]-**6**). Analogously, *N*-(pyridin-2-ylmethylene)propan-2-amine (**L7**) ligand is treated with $[(\eta^5\text{-}C_5H_5)Ru(PPh_3)_2Cl]$ to afford η^5-Cp−Ru(II)−*N*-isopropylpyridylimine complex, $[(\eta^5\text{-}C_5H_5)Ru(\kappa^2\text{-L7})PPh_3]^+$ ([**Ru**]-**7**). All the complexes [**Ru**]-**1**−[**Ru**]-**7** are highly stable in air and moisture. The spectroanalytical analyses of the synthesized complexes corroborated the proposed structures well (see the Experimental Section).

In the ^{1}H NMR spectra of the complexes [**Ru**]-**1**−[**Ru**]-**6**, the ortho C−H of pyridylamine resonated at 8.61−8.32 ppm in comparison to those of free ligands (8.50−8.29 ppm). Analogously, the ortho C−H of complex [**Ru**]-**7** resonated in a downfield region (9.28 ppm) in comparison to free ligand **L7** (8.63 ppm). The observed downfield shift is consistent with the coordination of pyridylamine/pyridylimine ligands with the η^5-Cp−Ru(II) moiety.[17,18] The observed downfield shift in the resonance of the aromatic C−H proton of PPh_3 in the ^{1}H NMR region of 7.49−6.94 ppm along with the appearance of a sharp singlet in ^{31}P NMR (55.33−53.17 ppm in [**Ru**]-**1** - [**Ru**]-**6** and 48.18 ppm in [**Ru**]-**7**) is in accordance with the coordination of PPh_3 to η^5-Cp−Ru(II).[17,18,33−35] Moreover, the Ru(II)-coordinated η^5-Cp proton resonated as a sharp singlet in the range of 4.80−4.30 ppm. In addition, the counteranion PF_6 resonated at ∼−144 ppm in ^{31}P NMR for these complexes.[18]

Further, molecular structures of the complexes [**Ru**]-**1**−[**Ru**]-**7** have all been authenticated by X-ray crystallography (Figure 1 and Table 1). The important bond parameters are shown in Table 2 (Tables S1 and S2 in the Supporting Information). The complexes [**Ru**]-**1**, [**Ru**]-**4**, [**Ru**]-**6**, and [**Ru**]-**7** crystallized in a monoclinic crystal system with $P2_1/n$ space group ($I2/a$ space group for [**Ru**]-**4**), whereas complexes [**Ru**]-**2** and [**Ru**]-**3** crystallized in a triclinic crystal system with space group $P\bar{1}$. While the crystallographic refinement data for complex [**Ru**]-**5** are not satisfactory for reporting, they are consistent with the proposed structure of the complex [**Ru**]-**5** (Figure S1 and Tables S3 and S4 in the Supporting Information). All the complexes [**Ru**]-**1**−[**Ru**]-**7** adopted a typical three-legged *piano-stool* geometry around the Ru(II) center. In this *piano-stool* arrangement the κ^2 pyridylamine/pyridylimine and PPh_3 ligands occupied three legs of the stool, and the η^5-Cp ring is placed at the apex of the stool. For the η^5-Cp−Ru(II) moiety, the average Ru−C distances are in the range 2.157−2.203 Å, whereas Ru to η^5-Cp centroid distances are in the range of 1.817−1.877 Å.[5,17,18,36−38] The Ru−P distances are observed in the range of 2.300−2.345 Å, which is in accordance with the Ru−P distances reported for other related systems.[5,17,18,36−38] The Ru−N_{py} bonds (2.114−2.064 Å) and Ru−N_{imine} bond (2.055 Å in [**Ru**]-**7**) are slightly shorter than the Ru−N_{amine} bonds (2.198−2.144 Å).[5,17,18,33] In the complexes [**Ru**]-**1**−[**Ru**]-**7**, the N_{py}−Ru−$N_{amine/imine}$ angles are in the range of 75.5−77.6°, whereas $N_{py/amine/imine}$−Ru−P angles are in the range of ca. 94°. The η^5-Cp_{ct}−Ru−P/N angle of ca. 125° is consistent with the piano-*stool* geometry of the η^5-Cp−Ru(II)−pyridylamine/imine complexes. Summation of all the angles around N_{imine} is 359.67° for the complex [**Ru**]-**7**, which is in agreement with the planar iminic N_{imine}. Further, the planar arrangement of the pyridylimine ligand in the complex [**Ru**]-**7** is also well supported by the lowest torsion angle (−3.0(4)°) around N_{imine}. Notably, the iminic C═N is shorter (1.282 Å) in [**Ru**]-**7** in comparison to the C−N_{amine} bonds (1.440−1.488 Å) in complexes [**Ru**]-**1**−[**Ru**]-**6**.

Catalytic Transformation of Furan Derivatives to Levulinic Acid and Diketones in Water. Catalytic performance

DOI: 10.1021/acs.inorgchem.8b00536
Inorg. Chem. XXXX, XXX, XXX−XXX

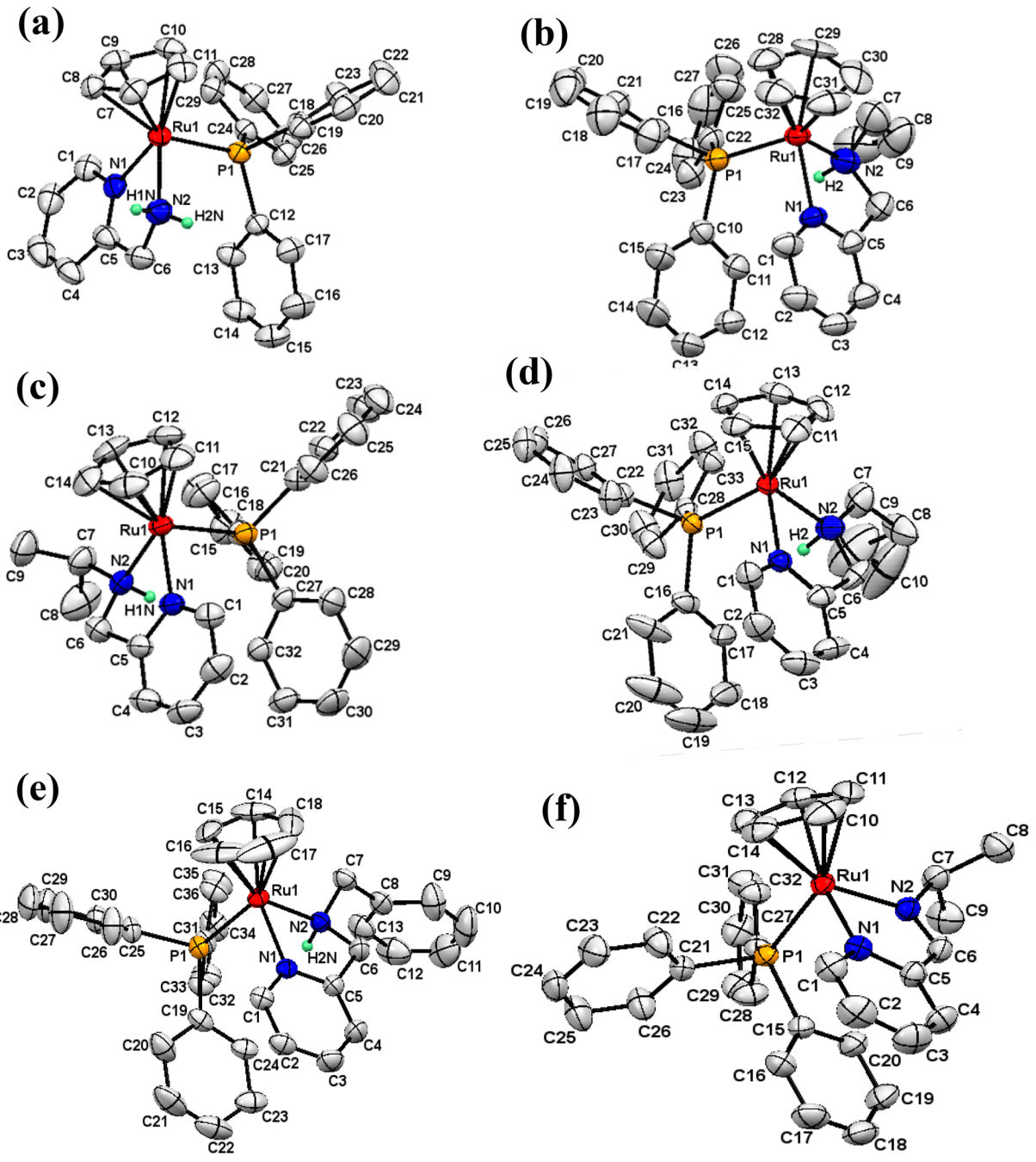

Figure 1. Single-crystal X-ray structures of complexes (a) [**Ru**]-**1**, (b) [**Ru**]-**2**, (c) [**Ru**]-**3**, (d) [**Ru**]-**4**, (e) [**Ru**]-**6**, and (f) [**Ru**]-**7**, with thermal ellipsoids at 30% probability. The anionic counterpart (PF_6) and hydrogen atoms, except for those on the amine nitrogen, are omitted for the sake of clarity.

of the synthesized η^5-Cp−Ru(II)−pyridylamine complexes [**Ru**]-**1**−[**Ru**]-**6** along with η^5-Cp−Ru(II)−pyridylimine complex [**Ru**]-**7** for the transformation of biomass-derived furans has been evaluated using furfural (**1a**) as the model substrate (as shown in Table 3) at 120 °C in the presence of 12 equiv of formic acid in water.

As elaborated in Table 3, complex [**Ru**]-**1** containing (2-pyridylmethyl)amine (**L1**) exhibited a 70% yield of LA (**1b**) in 6 h (Table 3, entry 1). An enhancement in the yield of LA (**1b**) to 84% is achieved by performing the catalytic reaction over the N_{amine}-*n*-propyl-substituted pyridylamine (**L2**) coordinated η^5-Cp−Ru(II) complex ([**Ru**]-**2**) (Table 3, entry 2). However, using η^5-Cp−Ru(II) containing various other N_{amine}-substituted pyridylamine ligands, (N_{amine}-isopropyl, [**Ru**]-**3**; N_{amine}-*n*-butyl, [**Ru**]-**4**; N_{amine}-isopentyl, [**Ru**]-**5**; N_{amine}-benzyl, [**Ru**]-**6**), the yield of LA (72−78%) could not be further enhanced (Table 3, entries 3−6). In contrast to the high catalytic activity of η^5-Cp−Ru(II) pyridylamine complexes, [**Ru**]-**7** having a rigid pyridylimine ligand displayed only 48% yield of LA under analogous reaction conditions (Table 3, entry 7). Notably, the precursor $[(\eta^5\text{-}C_5H_5)Ru(PPh_3)_2Cl]$ also exhibited a poor yield of LA (Table 3, entry 8). The lower catalytic activity of complex [**Ru**]-**1** is presumably due to the involvement of N_{amine} in strong interactions with solvent water molecules. Further it should be noted that, with an increase in alkyl carbon chain length or branching, the polarizability of N_{amine} also increases.[36] However,

DOI: 10.1021/acs.inorgchem.8b00536
Inorg. Chem. XXXX, XXX, XXX−XXX

Table 1. Crystal Data and Structure Refinement Details for [Ru]-1−[Ru]-4, [Ru]-6, and [Ru]-7

cryst param	[Ru]-1	[Ru]-2	[Ru]-3	[Ru]-4	[Ru]-6	[Ru]-7
empirical formula	$C_{29}H_{28}F_6N_2P_2Ru$	$C_{32}H_{34}F_6N_2P_2Ru$	$C_{32}H_{34}F_6N_2P_2Ru$	$C_{33}H_{35}F_6N_2P_2Ru$	$C_{36}H_{34}F_6N_2P_2Ru$	$C_{32}H_{32}F_6N_2P_2Ru$
formula wt	681.54	723.62	723.62	736.64	771.66	721.60
T (K)	293(2)	293(2)	293(2)	293(2)	293(2)	293(2)
λ (Å)	0.71073	1.54184	0.71073	1.54184	0.71073	0.71073
cryst syst	monoclinic	triclinic	triclinic	monoclinic	monoclinic	monoclinic
space group	$P2_1/c$	$P\bar{1}$	$P\bar{1}$	$I2/a$	$P2_1/n$	$P2_1/c$
cryst size (mm) ($l \times k \times h$)	0.23 × 0.16 × 0.11	0.33 × 0.26 × 0.18	0.23 × 0.18 × 0.13	0.33 × 0.26 × 0.21	0.19 × 0.16 × 0.12	0.19 × 0.13 × 0.10
a (Å)	8.2076(3)	9.7692(5)	9.8166(5)	21.1141(4)	11.2831(2)	9.7656(2)
b (Å)	17.4015(6)	10.9629(4)	10.7718(6)	9.7185(2)	16.6360(3)	19.6486(3)
c (Å)	19.0812(6)	16.8216(6)	16.7537(8)	32.6092(8)	19.5789(4)	16.4536(3)
α (deg)	90	74.993(3)	75.303(4)	90	90	90
β (deg)	94.399(3)	84.403(4)	83.477(4)	99.930(2)	104.828(2)	100.074(2)
γ (deg)	90	65.684(5)	65.615(5)	90	90	90
V (Å^3)	2717.23(16)	1585.67(13)	1560.67(15)	6591.1(2)	3552.68(12)	3108.45(10)
Z	4	2	2	8	4	4
ρ_{calcd} (g cm^{-3})	1.666	1.516	1.540	1.485	1.443	1.542
μ (mm^{-1})	0.759	5.486	0.666	5.290	0.590	0.669
$F(000)$	1376	736	736	3000	1568	1464
θ range (deg)	3.020−28.822	4.714−71.298	2.901−28.813	4.252−71.326	3.101−29.128	2.964−28.814
limiting indices	$-11 \le h \le 10$, $-23 \le k \le 23$, $-24 \le l \le 25$	$-11 \le h \le 11$, $-13 \le k \le 9$, $-20 \le l \le 17$	$-10 \le h \le 13$, $-14 \le k \le 13$, $-22 \le l \le 19$	$-25 \le h \le 19$, $-10 \le k \le 11$, $-39 \le l \le 39$	$-13 \le h \le 15$, $-20 \le k \le 22$, $-26 \le l \le 25$	$-13 \le h \le 12$, $-23 \le k \le 26$, $-20 \le l \le 21$
completeness to θ_{max} (%)	99.8	99.1	99.8	100.0	99.8	99.8
refinement method	full-matrix least squares on F^2					
no. of data collected/ unique data	24100/6443 (R(int) = 0.0715)	10073/5962 (R(int) = 0.0389)	14619/7124 (R(int) = 0.0284)	22414/6348 (R(int) = 0.0463)	34313/8518 (R(int) = 0.0324)	24722/7347 (R(int) = 0.0310)
no. of params/ restraints	369/0	388/0	394/1	397/0	428/0	338/0
goodness of fit on F^2	1.077	1.050	1.058	1.086	1.047	1.035
final R indices ($I > 2\sigma(I)$)	R1 = 0.0635, wR2 = 0.1570	R1 = 0.0572, wR2 = 0.1607	R1 = 0.0353, wR2 = 0.0940	R1 = 0.0657, wR2 = 0.1753	R1 = 0.0431, wR2 = 0.1086	R1 = 0.0416, wR2 = 0.1076
R indices (all data)	R1 = 0.0350, wR2 = 0.1647	R1 = 0.0578, wR2 = 0.1615	R1 = 0.0390, wR2 = 0.0978	R1 = 0.0679, wR2 = 0.1775	R1 = 0.0522, wR2 = 0.1163	R1 = 0.0473, wR2 = 0.1128
largest diff peak and hole (e Å^{-3})	1.910 and −1.723	0.925 and −1.440	0.600 and −0.530	2.548 and −0.616	0.975 and −0.694	0.847 and −0.927

DOI: 10.1021/acs.inorgchem.8b00536
Inorg. Chem. XXXX, XXX, XXX−XXX

Table 2. Important Bond Lengths (Å), Bond Angles (deg), and Torsion Angles (deg) for Complexes [Ru]-1−[Ru]-4, [Ru]-6, and [Ru]-7

	[Ru]-1	[Ru]-2	[Ru]-3	[Ru]-4	[Ru]-6	[Ru]-7
			Bond Lengths (Å)			
$Ru-C_t$	1.877	1.826	1.829	1.817	1.829	1.852
$Ru-C_{avg.}$	2.191	2.176	2.182	2.170	2.151	2.203
$Ru-N_{py}$	2.114(4)	2.104(3)	2.0936(19)	2.096(5)	2.105(2)	2.097(2)
$Ru-N_{amine/imine}$	2.163(4)	2.175(4)	2.198(2)	2.144(5)	2.185(2)	2.055(2)
Ru−P	2.3005(11)	2.3144(9)	2.3293(6)	2.3094(13)	2.3151(7)	2.3452(7)
$N_{amine/imine}-C_6$	1.475(6)	1.474(6)	1.485(3)	1.440(9)	1.488(4)	1.282(4)
$N_{amine/imine}$−C7		1.481(7)	1.523(3)	1.391(9)	1.504(3)	1.504(4)
			Bond Angles (deg)			
$N_{py}-Ru-N_{amine/imine}$	77.06(16)	77.64(14)	76.60(8)	77.6(2)	77.13(9)	76.29(9)
N_{py}−Ru−P	93.16(10)	90.15(9)	90.79(5)	91.22(12)	90.81(6)	88.08(6)
$N_{amine/imine}$−Ru−P	94.46(13)	92.66(11)	90.13(6)	92.9(2)	91.39(7)	90.74(7)
$N_{py}-Ru-C_t$	127.65	128.12	127.94	127.15	126.87	130.28
$N_{amine/imine}$-Ru-C_t	124.94	127.93	130.66	127.97	128.57	128.09
P−Ru−C_t	125.98	125.94	125.60	125.89	127.08	127.30
			Torsion Angles (deg)			
$N_{py}-C_5-C_6-N_{amine/imine}$	23.6(6)	−25.6(6)	32.6(3)	−15.3(9)	−30.2(4)	−3.0(4)

Table 3. Catalytic Activity of Cyclopentadienyl−Ruthenium(II) Complexes for Transformation of Furfural (1a) to Levulinic Acid (1b)[a]

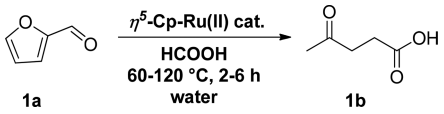

entry	catalyst	temp. (°C)	time (h)	HCOOH (mmol)	yield (%)[b]
1	[Ru]-1	120	6	12	70
2	[Ru]-2	120	6	12	84
3[c]	[Ru]-2	120	2, 4	12	35, 51
4[d]	[Ru]-2	60, 80, 100	6	12	0, 1, 21
5[e]	[Ru]-2	120	6	3, 6	50, 55
3	[Ru]-3	120	6	12	72
4	[Ru]-4	120	6	12	74
5	[Ru]-5	120	6	12	76
6	[Ru]-6	120	6	12	78
7	[Ru]-7	120	6	12	48
8	$[(\eta^5\text{-}C_5H_5)Ru(PPh_3)_2Cl]$	120	6	12	45

[a]Reaction conditions: furfural (1.0 mmol), formic acid (12 equiv), ruthenium catalyst (5 mol %), water (10 mL). [b]Yield determined by ^{1}H NMR with respect to the internal standard (*p*-anisaldehyde), [c]Effect of reaction time. [d]Effect of reaction temperature. [e]Effect of formic acid concentration.

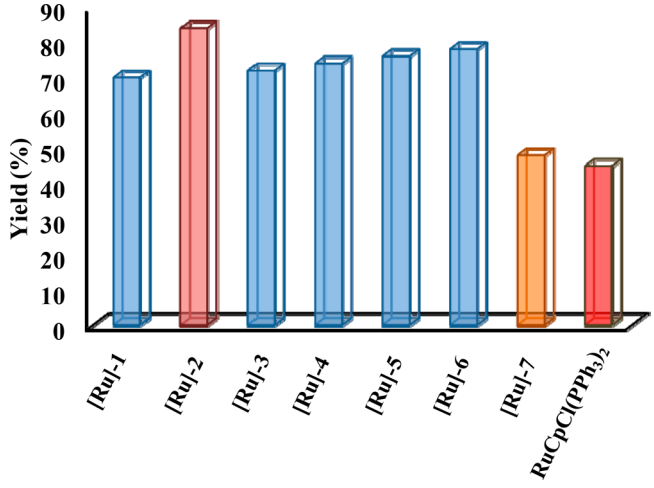

Figure 2. Catalytic transformation of furfural to LA by η^5-Cp−Ru(II) complexes in water. Reaction conditions: furfural (1.0 mmol), ruthenium catalyst (5 mol %), formic acid (12 equiv), and water (10 mL) at 120 °C for 6 h.

an increase in alkyl chain length may also increase the steric hindrance at the nitrogen center (N_{amine}), which may lead to a decrease in the basicity of nitrogen.[36] Further, the significantly enhanced catalytic efficiency of η^5-Cp−Ru(II) pyridylamine complexes **[Ru]-1**−**[Ru]-6** (70−84% yield of LA) in comparison to η^5-Cp−Ru(II) pyridylimine complex **[Ru]-7** (45% yield of LA) clearly evidenced the crucial role of the flexible pyridylamine ligands over the rigid pyridylimine ligand (Figure 2).[17,18,37] In this context, preceding studies suggested that pyridylphosphine- and aminophosphine-based hemilabile ligands may show flexible coordination behavior, which consequently create a vacant coordination site at the metal center.[17,18,37] Comparing the catalytic activity of various aminophosphine ligands, Weissensteiner et al. demonstrated that the flexible *N,N*-dimethyl-diphenylphosphinoethylamine (PN) exhibited the highest catalytic activity for the transfer hydrogenation of ketone to secondary alcohol in comparison to the rigid *N,N*-dimethyl-2-diphenylphosphinoaniline (DBD) and 2-{1-(*N,N*-dimethylamino)-ethyl}-1-diphenyl phosphinoferrocene (PPFA).[17] A similar dissociation and recoordination of the amine group was also observed for the flexible pyridylamine in a Pd−pyridylamine-catalyzed copolymerization of ethylene and norbornene.[37] Hence, on the basis of the aforementioned findings, we proposed that the ruthenium-bound κ^2-pyridylamine ligands in the complexes **[Ru]-1**−**[Ru]-6** may presumably undergo a reversible $\kappa^2-\kappa^1-\kappa^2$ coordination/decoordination interconversion, where the pyridyl group remains coordinated with the ruthenium and the amine branch is pendant.[37] This will create a new vacant site for the coordination of formate and subsequently form a Ru−H species to further facilitate the transfer hydrogenation of furfural (**1a**) to furfuryl alcohol. Further, the furfuryl alcohol undergoes an acid-assisted ring opening to LA (**1b**) (Figure S2 in the Supporting Information).

Further, the steric crowding at the N_{amine} center of the complexes **[Ru]-2**−**[Ru]-5** is estimated by comparing the N···C_n and N−H···C_n distances (where C_n is the farthest carbon of the

DOI: 10.1021/acs.inorgchem.8b00536
Inorg. Chem. XXXX, XXX, XXX−XXX

alkyl chain, and n ($n \geq 2$) represents the position of the carbon from the N_{amine}) obtained from their single-crystal X-ray structures (Figure S3 and Table S5 in the Supporting Information). The results implied that the methyl groups of the iso-propyl chain are placed very close to the N_{amine} ($N\cdots C_2$ 2.499 Å) in [**Ru**]-**3** in comparison to that in [**Ru**]-**2** ($N\cdots C_2$ 2.529 Å and $N\cdots C_3$ 3.251 Å), suggesting more crowding at N_{amine} in the complex [**Ru**]-**3**. Further, it is observed that the $N\cdots C_2$ distance in complex [**Ru**]-**2** is more than that in the complexes [**Ru**]-**4** and [**Ru**]-**5**, having bulky long carbon chains at N_{amine}, suggesting the least steric crowding at N_{amine} in complex [**Ru**]-**2**. Moreover, the $N-H\cdots C_n$ distances are also in good agreement with the observed trend in $N\cdots C_n$ distances (Table S5 in the Supporting Information). It is interesting to note that the $N\cdots C_3$ (3.251 Å) and $N-H\cdots C_3$ (2.873 Å) distances in the complex [**Ru**]-**2** are longer than those in the complex [**Ru**]-**4**, which clearly evidenced the relatively less steric crowding at N_{amine} of the complex [**Ru**]-**2**. Moreover, we also observed that the long isopentyl substituent at N_{amine} of the complex [**Ru**]-**5** can fold back and, hence, may cause steric crowding at N_{amine} (Figure S4 in the Supporting Information). Therefore, the basicity and the steric crowding at N_{amine} is also expected to play a crucial role in tuning the catalytic activity of the studied η^5-Cp−Ru(II) complexes for the transformation of furfural (**1a**) to LA (**1b**).[36]

Now, the high-performing [**Ru**]-**2** catalyst was used for further optimization of the catalytic reaction conditions for the transformation of furfural (**1a**) to LA (**1b**). Performing the reaction at a lower temperature (60−100 °C) resulted in a sharp decrease in the yield of LA (**1b**) (Table S6 in the Supporting Information). Moreover, decreasing the amount of formic acid to 3 or 6 equiv is also found to have a detrimental effect on the yield of LA (**1b**) (Table S7 in the Supporting Information). It should be noted that in the presence of catalyst alone (without formic acid), catalyst with H_2 gas, or without catalyst only with formic acid (12 equiv), the reaction could not proceed, suggesting the presence of formic acid and the catalyst together is essential to achieve an efficient transformation of furfural (**1a**) to LA (**1b**). Time-dependent reaction progress monitored in 2, 4, and 6 h displayed a gradual increase in the yield of LA (**1b**) from 35% (2 h) to 84% (6 h) (Table S8 in the Supporting Information).

Therefore, the catalytic performance of the high-performing complex [**Ru**]-**2** has also been further investigated for the transformation of other furan derivatives, 5-HMF (**2a**) and 5-MF (**3a**), under the optimized reaction conditions (catalyst 5 mol %, formic acid 12 equiv, at 120 °C, 6 h in water). Unlike furfural (**1a**), only 66% conversion of 5-HMF (**2a**) is achieved in 6 h. However, 96% conversion of 5-HMF (**2a**) to open-ring products 1-HHD (**2b**) with 69% selectivity (yield 42%) along with LA (**1b**) and 3-HHD (**3b**) (Scheme 3b) is observed for the reaction performed for longer duration (12 h). Formation of 1-HHD (**2b**) as the major open-ring product from 5-HMF (**2a**) has also been reported earlier with other catalytic systems such as Pd/C, Cp*Ir, and η^6-arene−Ru(II) complex.[21,23,27,28] Interestingly, reaction with 5-MF (**3a**) resulted in the formation of 3-HHD (**3b**, selectivity 84%) and 2,5-HD (**3c**, selectivity 16%) (Scheme 3c). Formation of 3-HHD (**3b**) as a major product over 2,5-HD (**3c**) is presumably due to the higher preference toward hydration over hydrogenation of the intermediate hex-3-ene-2,5-diene (HED).

Encouraged by the above results, catalytic transformation of fructose over [**Ru**]-**2** catalyst at 120 °C with 12 equiv of formic acid was also performed, which led to the formation of 1-HHD (**2b**), LA (**1b**), 2,5-HD (**3c**), and 5-HMF (**2a**) in 65%, 13%, 13% and 9% selectivities, respectively, in 6 h (Scheme 3d). Formation of 5-HMF (**2a**) and 1-HHD (**2b**) products from fructose is consistent with previous reports, suggesting that this transformation proceeded through the formation of platform dehydrogenated precursor 5-HMF (**2a**), which subsequently transformed to 1-HHD (**2b**).[38]

Notably, the recovered catalyst [**Ru**]-**2** (5 mol %) showed high stability and therefore could be recycled for four consecutive catalytic runs for the transformation of furfural (**1a**) to LA (**1b**), where a 60% yield of LA (**1b**) was achieved even after the fourth catalytic run (TON for first catalytic run 16.8 and TTN 58.4) (Figure S5 in the Supporting Information). Experiments performed in the presence of Hg metal showed no significant change in catalytic activity of [**Ru**]-**2** for furfural (**1a**) to LA (**1b**) transformation, suggesting that the active catalytic species is homogeneous in nature.[39] To further explore the practical applicability of this catalytic methodology, a gram-scale experiment was also carried out for the catalytic transformation of furfural over [**Ru**]-**2** catalyst (1 mol %) and achieved 64% yield of LA (**1b**) in 15 h (TON 64.0) (Scheme 3e).

Therefore, the above findings clearly evidenced the high stability of the [**Ru**]-**2** catalyst at high temperature (>120 °C) in water and in the presence of an acid (formic acid). Moreover, as inferred from the Hg poisoning experiments, no decomposition of [**Ru**]-**2** catalysts to Ru nanoparticles is observed under the catalytic reaction conditions (>120 °C in water). The observed high stability of [**Ru**]-**2** catalysts can be attributed to the strong coordination of η^5-Cp to the Ru center, while η^6-arene−Ru(II) complexes decomposed to Ru nanoparticles at

Scheme 3. Catalytic Transformation of Different Bio-Derived Furans over [Ru]-2 Catalyst

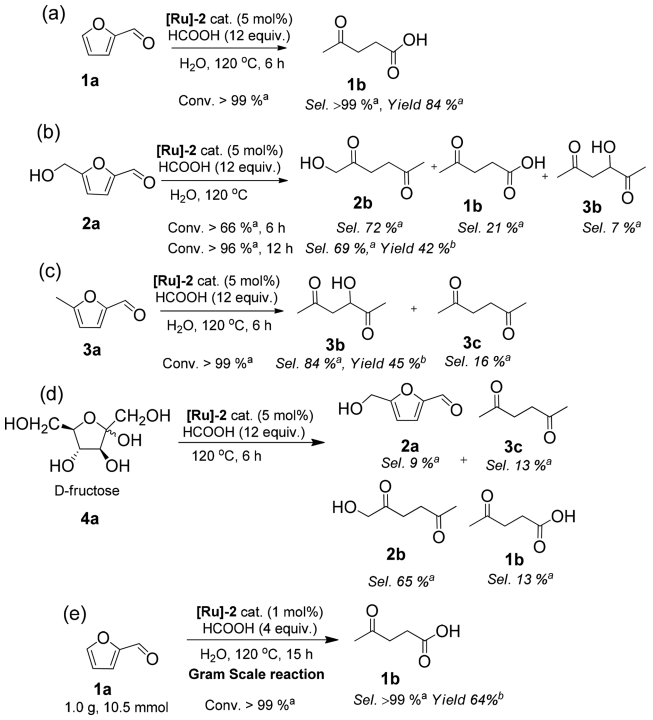

[a]determined by ^{1}H NMR with respect to the internal standard (*p*-anisaldehyde), [b]determined by ^{1}H NMR of the purified product obtained from column chromatography (ethyl acetate/hexane 2/98−10/90 v/v).

DOI: 10.1021/acs.inorgchem.8b00536
Inorg. Chem. XXXX, XXX, XXX−XXX

a higher temperature.[29,30] Moreover, the high aqueous and thermal stability of the studied η^5-Cp−Ru(II)−pyridylamine complexes is also reflected in their two-fold higher catalytic activity (84% yield of LA, 6 h, 120 °C, 12 mmol of HCOOH) over the analogous η^6-arene−Ru(II) (42% yield of LA, 8 h, 100 °C, 12 mmol of HCOOH).[27] Notably, previously explored catalysts based on a η^5-Cp*−Ir complex or other metal nanoparticle catalysts (Pd/Al_2O_3 or Au/Nb_2O_5) required high H_2 gas pressure (5−80 bar) and higher temperature (120−170 °C) for analogous catalytic transformations (Table S9 in the Supporting Information).[19−26] Therefore, the studied η^5-Cp−Ru(II)−pyridylamine complexes represent a class of highly active catalysts with high thermal and aqueous stability, showing catalytic activity higher than or on par with that of previously reported catalytic systems.

CONCLUSIONS

In summary, we synthesized and characterized (by ^{1}H, ^{13}C, ^{31}P, NMR, and mass) a series of cationic η^5-Cp−Ru(II)−pyridylamine ([**Ru**]-**1**−[**Ru**]-**6**) and η^5-Cp−Ru−pyridylimine ([**Ru**]-7) complexes and authenticated the molecular structures of all the complexes by X-ray crystallography. The synthesized η^5-Cp−Ru−pyridylamine complexes displayed high catalytic activity for the transformation of the biomass-derived furans, furfural (**1a**), 5-HMF (**2a**), and 5-MF (**3a**) to the value-added open-ring products, LA (**1b**) and diketones (1-HHD (**2b**), 3-HHD (**3b**) and 2,5-HD (**3c**)) with high conversion (>99%) and selectivity at 120 °C in the presence of formic acid. Experimental findings demonstrated that the η^5-Cp−Ru−pyridylamine complexes exhibited higher catalytic performance in comparison to the analogous η^5-Cp−Ru−pyridylimine complex, which can be attributed to the hemilabile nature of the pyridylamine ligands and the basicity and bulkiness at N_{amine}. Moreover, the studied catalytic system has also been applied to the transformation of fructose and the gram-scale transformation of furfural to open-ring products for practical applications. Therefore, the high catalytic activity along with the aqueous and thermal stability demonstrated by the studied η^5-Cp−Ru(II) complexes may also find applications in various other high-temperature catalytic reactions.

EXPERIMENTAL SECTION

Procedure for the Synthesis of Cyclopentadienyl-Ruthenium-(II) Complexes [Ru]-1−[Ru]-7. Complexes [**Ru**]-**1**−[**Ru**]-7 were synthesized by treating N-substituted pyridylamine (**L1**−**L6**) and pyridylimine (**L7**) ligands with the cyclopentadienyl−ruthenium precursor $[(\eta^5\text{-}C_5H_5)RuCl(PPh_3)_2]$ in methanol (25 mL) under reflux conditions for 20 h. Later, the volume was reduced to 10 mL, and then NH_4PF_6 was added (0.489 g, 3.0 mmol). The resulting solution was stirred for 12 h at room temperature to obtain the desired complexes as precipitates, which were washed with diethyl ether (3 × 10 mL) and dried in air.

*Synthesis of $[(\eta^5\text{-}C_5H_5)RuPPh_3(\kappa^2\text{-}(N,N)\text{-}2\text{-}(aminomethyl)pyridine]PF_6$ ([**Ru**]-**1**).* Complex [**Ru**]-**1** iswas synthesized following the above general procedure, by using 2-(aminomethyl)pyridine (**L1**) (1.180 g, 1.1 mmol) and $[(\eta^5\text{-}C_5H_5)Ru(PPh_3)_2Cl]$ (0.363 g, 0.5 mmol). Pale yellow solid, yield 0.210 g (61%). FTIR (ν, cm^{-1}): 3357, 3313 ν(N−H stretching), 1606 ν(N−H bending), 1090 ν(C−N), 832 ν(PF_6 stretching), 556 ν(PF_6 bending). ^{1}H NMR (400 MHz, DMSO-d_6): δ (ppm) 8.61 (d, 1H, J = 5.20 Hz), 7.56 (t, 1H, J_1 = 7.80 Hz, J_2 = 7.52 Hz), 7.39 (t, 6H, J_1 = 9.28 Hz, J_2 = 6.24 Hz), 7.32 (t, 6H, J_1 = 8.80 Hz, J_2 = 6.28 Hz), 7.28 (d, 1H, J = 8.28 Hz), 7.12 (t, 6H, J_1 = 9.28 Hz, J_2 = 8.04 Hz), 6.79 (t, 1H, J_1 = 6.52 Hz, J_2 = 6.28 Hz), 4.36 (s, 5H), 4.03−3.99 (m, 1H). ^{13}C NMR (100 MHz, DMSO-d_6): δ (ppm) 162.28, 155.77, 136.18, 134.35, 133.97, 132.97, 132.86, 129.64, 128.32, 128.23, 123.02, 120.32, 75.09, 53.54. ^{31}P NMR (161.97 MHz, DMSO-d_6): δ (ppm) 55.33 (s, PPh_3), −144.19 (sep, PF_6). MS (ESI): m/z calculated for $[(\eta^5\text{-}C_5H_5)Ru(\kappa^2\text{-}$**L1**$)PPh_3]^+$ (**L1** = 2-(aminomethyl) pyridine) 537.1 $[M]^+$, found 537.1 $[M]^+$. UV−vis (dichloromethane, λ_{max}, nm (ε, M^{-1} cm^{-1})): 365 (3.7 × 10^3), 327 (6.8 × 10^3), 274 (8.0 × 10^3), 267 (7.1 × 10^3). The CCDC deposition number of the complex [**Ru**]-**1** is 1564514.

*Synthesis of $[(\eta^5\text{-}C_5H_5)RuPPh_3(\kappa^2\text{-}(N,N)\text{-}N\text{-}(pyridin\text{-}2\text{-}ylmethyl)propan\text{-}1\text{-}amine]PF_6$ ([**Ru**]-**2**).* Complex [**Ru**]-**2** was synthesized following the above general procedure, by using *N*-(pyridin-2-ylmethyl)propan-1-amine (**L2**) (0.165 g, 1.1 mmol) and $[(\eta^5\text{-}C_5H_5)Ru(PPh_3)_2Cl]$ (0.363 g, 0.5 mmol). Pale yellow solid, yield 0.225 g (62%). FTIR (ν, cm^{-1}): 3277 ν(N−H stretching), 1605 ν(N−H bending), 1091 ν(C−N), 833 ν(PF_6 stretching), 557 ν(PF_6 bending). ^{1}H NMR (400 MHz, DMSO-d_6): δ (ppm) 8.39 (d, 1H, J = 5.24 Hz), 7.70 (t, 1H, J_1 = 7.76 Hz, J_2 = 7.52 Hz), 7.46 (t, 3H, J_1 = 6.28 Hz, J_2 = 8.28 Hz), 7.42 (d, 1H, J = 7.76 Hz), 7.39 (t, 6H, J = 7.56 Hz, J_2 = 7.00 Hz), 7.00 (t, 6H, J_1 = 9.28 Hz, J_2 = 8.28 Hz), 6.90 (t, 1H, J_1 = 6.52 Hz, J_2 = 6.52 Hz), 4.51 (s, 5H), 4.39 (dd, 1H, J_1 = 15.56 Hz, J_2 = 15.56 Hz), 4.09−4.02 (m, 1H), 3.29−3.25 (m, 1H), 3.19−3.14 (m, 1H), 2.90−2.88 (m, 1H), 1.40−1.36 (m, 1H), 1.18−1.15 (m, 1H), 0.54 (t, 3H, J_1 = 7.28 Hz, J_2 = 7.52 Hz). ^{13}C NMR (100 MHz, DMSO-d_6): δ (ppm) 161.23, 155.37, 136.74, 132.99, 132.77, 132.65, 132.61, 130.07, 128.76, 128.67, 123.55, 120.92, 75.68, 61.13, 60.71, 21.49, 10.29. ^{31}P NMR (161.97 MHz, DMSO-d_6): δ (ppm) 54.98 (s, PPh_3), −144.19 (sep, PF_6). MS (ESI): m/z calculated for $[(\eta^5\text{-}C_5H_5)Ru(\kappa^2\text{-}$**L2**$)PPh_3]^+$ (**L2** = *N*-(pyridin-2-ylmethyl)propan-1-amine) 579.1 $[M]^+$, found 579.1 $[M]^+$. UV−vis (dichloromethane, λ_{max}, nm (ε, M^{-1} cm^{-1})): 369 (3.7 × 10^3), 329 (6.7 × 10^3), 274 (7.5 × 10^3), 266 (6.6 × 10^3). The CCDC deposition number of the complex [**Ru**]-**2** is 1556948.

*Synthesis of $[(\eta^5\text{-}C_5H_5)RuPPh_3(\kappa^2\text{-}(N,N)\text{-}N\text{-}(pyridin\text{-}2\text{-}ylmethyl)propan\text{-}2\text{-}amine]PF_6$ ([**Ru**]-**3**).* Complex [**Ru**]-**3** was synthesized following the above general procedure, by using *N*-(pyridin-2-ylmethyl)-propan-2-amine (**L3**) (0.165 g, 1.1 mmol) and $[(\eta^5\text{-}C_5H_5)Ru(PPh_3)_2Cl]$ (0.363 g, 0.5 mmol). Pale yellow solid, yield 0.240 g (66%). FTIR (ν, cm^{-1}): 3274 ν(N−H stretching), 1604 ν(N−H bending), 1093 ν(C−N), 828 ν(PF_6 stretching), 556 ν(PF_6 bending). ^{1}H NMR (400 MHz, DMSO-d_6): δ (ppm) 8.16 (d, 1H, J = 5.24 Hz), 7.76 (t, 1H, J_1 = 7.60 Hz, J_2 = 7.76 Hz), 7.50 (t, 3H, J_1 = 7.56 Hz, J_2 = 7.00 Hz), 7.48 (d, 1H, J = 7.75 Hz), 7.44 (t, 6H, J_1 = 6.28 Hz, J_2 = 8.52 Hz), 7.00 (t, 6H, J_1 = 8.80 Hz, J_2 = 8.28 Hz), 6.94 (t, 1H, J_1 = 6.28 Hz, J_2 = 7.04 Hz), 4.64 (s, 5H), 4.14−4.11 (m, 1H), 3.26−3.21 (m, 1H), 1.94−1.88 (m, 1H), 0.93 (dd, 6H, J_1 = 6.04 Hz, J_2 = 6.52 Hz). ^{13}C NMR (100 MHz, DMSO-d_6): δ (ppm) 161.55, 154.93, 137.10, 132.82, 132.73, 132.63, 132.44, 130.27, 128.99, 128.90, 123.42, 121.08, 75.33, 58.35, 56.63, 24.72, 20.48. ^{31}P NMR (161.97 MHz, DMSO-d_6): δ (ppm) 54.44 (s, PPh_3), −144.17 (sep, PF_6). MS (ESI) m/z calculated for $[(\eta^5\text{-}C_5H_5)Ru(\kappa^2\text{-}$**L3**$)PPh_3]^+$ (**L3** = *N*-(pyridin-2-ylmethyl)propan-2-amine) 579.2 $[M]^+$, 579.2 found $[M]^+$. UV−vis (dichloromethane, λ_{max}, nm (ε, M^{-1} cm^{-1})): 369 (3.7 × 10^3), 329 (6.9 × 10^3), 275 (7.7 × 10^3), 266 (6.7 × 10^3). The CCDC deposition number of the complex [**Ru**]-**3** is 1564515.

*Synthesis of $[(\eta^5\text{-}C_5H_5)RuPPh_3(\kappa^2\text{-}(N,N)\text{-}N\text{-}(pyridin\text{-}2\text{-}ylmethyl)butan\text{-}1\text{-}amine]PF_6$ ([**Ru**]-**4**).* Complex [**Ru**]-**4** was synthesized following the above general procedure, by using *N*-(pyridin-2-ylmethyl)-butan-1-amine (**L4**) (0.180 g, 1.1 mmol) and $[(\eta^5\text{-}C_5H_5)Ru(PPh_3)_2Cl]$ (0.363 g, 0.5 mmol). Pale yellow solid, yield 0.250 g (67%). FTIR (ν, cm^{-1}): 3127 ν(N−H stretching), 1601 ν(N−H bending), 1092 ν(C−N), 830 ν(PF_6 stretching), 557 ν(PF_6 bending). ^{1}H NMR (400 MHz, DMSO-d_6): δ (ppm) 8.38 (d, 1H, J = 5.28 Hz), 7.70 (t, 1H, J_1 = 7.52 Hz, J_2 = 7.52 Hz), 7.45 (t, 3H, J_1 = 6.00 Hz, J_2 = 6.80 Hz), 7.39 (t, 6H, J_1 = 6.52 Hz, J_2 = 8.04 Hz), 7.19 (t, 1H, J_1 = 9.04 Hz, J_2 = 7.28 Hz), 7.00 (t, 6H, J_1 = 9.28 Hz, J_2 = 8.28 Hz), 6.89 (t, 1H, J_1 = 6.52 Hz, J_2 = 6.52 Hz), 4.51 (s, 5H), 4.42−4.37 (m, 1H), 4.11−4.03 (m, 1H), 3.24−3.22 (m, 1H), 2.91−2.85 (m, 1H), 1.36−1.31 (m, 1H), 1.18−1.10 (m, 1H), 0.96−0.91 (m, 1H), 0.77 (t, 3H, J_1 = 7.04 Hz, J_2 = 7.24 Hz). ^{13}C NMR (100 MHz, DMSO-d_6): δ (ppm) 161.23, 155.36, 136.75, 133.02, 132.77, 132.65, 130.06, 128.75, 128.65, 123.55, 120.92, 75.70, 60.88, 59.17, 30.53, 18.78,

DOI: 10.1021/acs.inorgchem.8b00536
Inorg. Chem. XXXX, XXX, XXX−XXX

13.66. ^{31}P NMR (161.97 MHz, DMSO-d_6): δ (ppm) 54.89 (s, PPh_3), −144.18 (sep, PF_6). MS (ESI): m/z calculated for $[(\eta^5\text{-}C_5H_5)Ru(\kappa^2\text{-}\mathbf{L4})PPh_3]^+$ (**L4** = N-(pyridin-2-ylmethyl)butan-1-amine) 593.2 $[M]^+$, found 593.2 $[M]^+$. UV−vis (dichloromethane, λ_{max}, nm (ε, M^{-1} cm^{-1})): 369 (3.5×10^3), 330 (5.9×10^3), 274 (7.9×10^3), 266 (7.0×10^3). The CCDC deposition number of the complex [**Ru**]-**4** is 1556949.

Synthesis of $[(\eta^5\text{-}C_5H_5)RuPPh_3(\kappa^2\text{-}(N,N)\text{-}3\text{-methyl-}N\text{-(pyridin-2-ylmethyl)butan-1-amine}]PF_6$ ([Ru]-5). Complex [**Ru**]-**5** was synthesized following the above general procedure, by using 3-methyl-*N*-(pyridin-2-ylmethyl)butan-1-amine (**L5**) (0.195 g, 1.1 mmol) and $[(\eta^5\text{-}C_5H_5)Ru(PPh_3)_2Cl]$ (0.363 g, 0.5 mmol). Pale yellow solid, yield 0.255 g (68%). FTIR (ν, cm^{-1}): 3306 ν(N−H stretching), 1608 ν(N−H bending), 1089 ν(C−N), 829 ν(PF_6 stretching), 556 ν(PF_6 bending). ^{1}H NMR (400 MHz, DMSO-d_6): δ (ppm) 8.37 (d, 1H, J = 5.16 Hz), 7.69 (t, 1H, J_1 = 7.76 Hz, J_2 = 9.04 Hz), 7.46 (t, 3H, J_1 = 7.52 Hz, J_2 = 5.76 Hz), 7.38 (t, 6H, J_1 = 6.28 Hz, J_2 = 7.04 Hz), 7.19 (t, 1H, J_1 = 9.04 Hz, J_2 = 8.04 Hz), 7.01 (t, 6H, J_1 = 9.00 Hz, J_2 = 8.28 Hz), 6.88 (t, 1H, J_1 = 6.28 Hz, J_2 = 6.52 Hz), 4.52 (s, 5H), 4.41 (dd, 1H, J_1 = 7.76 Hz, J_2 = 4.52 Hz), 4.11−4.04 (m, 1H), 3.24−3.21 (m, 1H), 1.28−1.19 (m, 2H), 1.11−0.98 (m, 1H), 0.80 (d, 3H, J = 6.28 Hz), 0.76 (d, 3H, J = 6.28 Hz). ^{13}C NMR (100 MHz, DMSO-d_6): δ (ppm) 161.23, 155.44, 136.74, 133.10, 132.78, 132.72, 132.67, 130.03, 128.72, 128.62, 123.54, 120.88, 75.71, 61.17, 57.79, 37.73, 25.04, 22.56, 22.33. ^{31}P NMR (161.97 MHz, DMSO-d_6): δ (ppm) 54.73 (s, PPh_3), −144.18 (sep, PF_6). MS (ESI) m/z calculated for $[(\eta^5\text{-}C_5H_5)Ru(\kappa^2\text{-}\mathbf{L5})PPh_3]^+$ (**L5** = 3-methyl-*N*-(pyridin-2-ylmethyl)butan-1-amine) 607.2 $[M]^+$, found 607.2 $[M]^+$. UV−vis (dichloromethane, λ_{max}, nm (ε, M^{-1} cm^{-1})): 363 (3.7×10^3), 329 (6.1×10^3), 274 (8.2×10^3), 267 (7.4×10^3). The CCDC deposition number of the complex [**Ru**]-**5** is 1564516.

Synthesis of $[(\eta^5\text{-}C_5H_5)RuPPh_3(\kappa^2\text{-}(N,N)\text{-}N\text{-benzyl-}1\text{-(pyridin-2-yl)methanamine}]PF_6$ ([Ru]-6). Complex [**Ru**]-**6** was synthesized following the above general procedure, by using *N*-benzyl-1-(pyridin-2-yl)methanamine (**L6**) (0.217 g, 1.1 mmol) and $[(\eta^5\text{-}C_5H_5)Ru(PPh_3)_2Cl]$ (0.363 g, 0.5 mmol). Pale yellow solid, yield 0.251 g (65%). FTIR (ν, cm^{-1}): 3254 ν(N−H stretching), 1605 ν(N−H bending), 1090 ν(C−N), 836 ν(PF_6 stretching), 557 ν(PF_6 bending). ^{1}H NMR (400 MHz, DMSO-d_6): δ (ppm) 8.36 (d, 1H, J = 5.28 Hz), 7.68 (t, 1H, J_1 = 9.28 Hz, J_2 = 7.76 Hz), 7.49 (t, 3H, J_1 = 7.52 Hz, J_2 = 7.00 Hz), 7.41 (t, 6H, J_1 = 6.24 Hz, J_2 = 8.56 Hz), 7.34−7.26 (m, 5H), 7.18−7.12 (m, 1H), 6.94 (t, 6H, J_1 = 9.32 Hz, J_2 = 8.00 Hz), 6.79 (d, 1H, J = 6.28 Hz), 4.61 (s, 5H), 4.50−4.46 (m, 1H), 4.39−4.33 (m, 1H), 4.27−4.20 (m, 1H), 3.95 (dd, 1H, J_1 = 4.52 Hz, J_2 = 4.52 Hz). ^{13}C NMR (100 MHz, DMSO-d_6): δ (ppm) 161.04, 155.48, 137.10, 136.69, 133.49, 133.38, 132.03, 132.98, 132.92, 132.60, 130.40, 129.15, 129.05, 128.90, 128.81, 128.41, 123.86, 121.37, 75.95, 62.87, 60.96. ^{31}P NMR (161.97 MHz, DMSO-d_6): δ (ppm) 55.317 (s, PPh_3), −144.18 (sep, PF_6). MS (ESI) m/z calculated for $[(\eta^5\text{-}C_5H_5)Ru(\kappa^2\text{-}\mathbf{L6})PPh_3]^+$ (**L6** = *N*-benzyl-1-(pyridin-2-yl)-methanamine) 627.2 $[M]^+$, found 626.8 $[M]^+$. UV−vis (dichloromethane, λ_{max}, nm (ε, M^{-1} cm^{-1})): 366 (2.9×10^3), 328 (5.3×10^3), 373 (7.2×10^3), 266 (6.6×10^3). The CCDC deposition number of the complex [**Ru**]-**6** is 1564517.

Synthesis of $[(\eta^5\text{-}C_5H_5)RuPPh_3(\kappa^2\text{-}(N,N)\text{-}N\text{-(pyridin-2-ylmethylene)propan-2-amine}]PF_6$ ([Ru]-7). Complex [**Ru**]-**7** was synthesized following the above general procedure, by using *N*-(pyridin-2-ylmethylene)propan-2-amine (**L7**) (0.162 g, 1.1 mmol) and $[(\eta^5\text{-}C_5H_5)Ru(PPh_3)_2Cl]$ (0.363 g, 0.5 mmol). Brown solid, yield 0.255 g (70%). FTIR (ν, cm^{-1}): 1092 ν(C−N), 830 ν(PF_6 stretching), 557 ν(PF_6 bending). ^{1}H NMR (400 MHz, DMSO-d_6): δ (ppm) 9.28 (d, 1H, J = 5.52 Hz), 8.63 (d, 1H, J = 5.03 Hz), 7.70 (t, 1H, J_1 = 7.80 Hz, J_2 = 7.52 Hz), 7.62 (d, 6H, J = 7.76 Hz), 7.43 (t, 3H, J_1 = 7.52 Hz, J_2 = 6.76 Hz), 7.36 (t, 6H, J_1 = 6.80 Hz, J_2 = 7.00 Hz), 7.19 (t, 1H, J_1 = 7.00 Hz, J_2 = 6.00 Hz), 7.02 (t, 6H, J_1 = 9.28 Hz, J_2 = 8.56 Hz), 4.84 (s, 5H), 4.66−4.59 (m, 1H), 1.42 (d, 3H, J = 6.56 Hz), 0.80 (d, 3H, J = 6.52 Hz). ^{13}C NMR (100 MHz, DMSO-d_6): δ (ppm) 160.69, 156.05, 155.68, 135.36, 132.71, 132.60, 131.36, 130.95, 130.13, 128.57, 128.47, 127.56, 124.45, 78.94, 66.29, 25.00, 21.63. ^{31}P NMR (161.97 MHz, DMSO-d_6): δ (ppm) 48.18 (s, PPh_3), −144.18 (sep, PF_6). MS (ESI) m/z calculated for $[(\eta^5\text{-}C_5H_5)Ru(\kappa^2\text{-}\mathbf{L7})PPh_3]^+$ (**L7** = *N*-(pyridin-2-ylmethylene)propan-2-amine) 577.1 $[M]^+$, found 577.1 $[M]^+$. UV−vis (dichloromethane, λ_{max}, nm (ε, M^{-1} cm^{-1})): 436/2.9 × 10^3, 337/2.5 × 10^3, 273/9.1 × 10^3, 267/8.0 × 10^3. CCDC deposition number of the complex [**Ru**]-**7** is 1564518.

General Procedure for η^5-Cp−Ru(II)-Catalyzed Transformation of Furfural (1a) and Its Derivatives to Levulinic Acid (1b) and Diketones in Water. All of the reactions were carried out in a Teflon-coated autoclave. To an aqueous suspension (10 mL) of η^5-Cp−Ru(II) catalyst (5 mol %) was added 1.0 mmol of furan (or its derivatives or fructose) and formic acid (as specified), and the reaction mixture was heated at 120 °C for the specified duration. After completion of the reaction, the reaction mixture was cooled to room temperature and dried under reduced pressure. The selectivity of the products was determined by ^{1}H NMR. The yield for LA (**1b**) from furfural (**1a**) was determined by isolating the purified product through column chromatography (ethyl acetate/hexane 2/98 to 10/90 v/v) and by ^{1}H NMR in $CDCl_3$ with reference to *p*-anisaldehyde added as an internal standard (Figure S7 in the Supporting Information). The yields of the diketone products 1-HHD (**2b**, from 5-HMF, **2a**) and 3-HHD (**3b**, from 5-MF, **3a**) were determined by isolating the purified products by column chromatography (ethyl acetate/hexane 2/98 to 10/90 v/v).

■ ASSOCIATED CONTENT

Supporting Information

The Supporting Information is available free of charge on the ACS Publications website at DOI: 10.1021/acs.inorgchem.8b00536.

Crystallographic data, catalyst tests, and characterization data (PDF)

Accession Codes

CCDC 1556948−1556949 and 1564514−1564518 contain the supplementary crystallographic data for this paper. These data can be obtained free of charge via www.ccdc.cam.ac.uk/data_request/cif, or by emailing data_request@ccdc.cam.ac.uk, or by contacting The Cambridge Crystallographic Data Centre, 12 Union Road, Cambridge CB2 1EZ, UK; fax: +44 1223 336033.

■ AUTHOR INFORMATION

Corresponding Author

*E-mail for S.K.S.: sksingh@iiti.ac.in.

ORCID

Shaikh M. Mobin: 0000-0003-1940-3822

Sanjay K. Singh: 0000-0002-8070-7350

Notes

The authors declare no competing financial interest.

■ ACKNOWLEDGMENTS

The authors thanks the IIT Indore, CSIR, New Delhi, and SERB (DST), New Delhi, for financial support. SIC, IIT Indore is acknowledged for instrumentation facilities. A.D.D. and V.K.S. thank the CSIR, New Delhi, and UGC, New Delhi, for their fellowships. A.D.D. and V.K.S. synthesized catalysts and performed the reactions, A.D.D. and S.K.S. designed the experiments and wrote the manuscript, and S.M.M. elucidated molecular structures of the complexes by single-crystal X-ray crystallography.

■ REFERENCES

(1) Ganter, C. Chiral organometallic half-sandwich complexes with defined metal configuration. *Chem. Soc. Rev.* **2003**, *32*, 130−138.

(2) (a) Kumar, P.; Gupta, R. K.; Pandey, D. S. Half-sandwich arene ruthenium complexes: synthetic strategies and relevance in catalysis. *Chem. Soc. Rev.* **2014**, *43*, 707−733. (b) Dodo, N.; Matsushima, Y.;

DOI: 10.1021/acs.inorgchem.8b00536
Inorg. Chem. XXXX, XXX, XXX−XXX

Uno, M.; Onitsuka, K.; Takahashi, S. Synthesis of ruthenium complexes with planar-chiral cyclopentadienyl-pyridine or -phosphine bidentate ligands. *J. Chem. Soc., Dalton Trans.* **2000**, 35−41. (c) Albers, M. O.; Robinson, D. J.; Singleton, E. The chemistry of cyclopentadienyl-ruthenium and -osmium complex II. Novel mononuclear cyclopentadienyl ruthenium complexes containing aromatic amine ligands. A facile synthetic route. *J. Organomet. Chem.* **1986**, *311*, 207−215. (d) de Klerk-Engels, B.; Delis, J. G. P.; Vrieze, K. Synthesis of Cyclopentadienyl-(1,4-diisopropyl-l,3-diazabutadie)(L))ruthenium trifluoromethanesulfonate (L = Alkene, Alkyne, CO, Pyridine, PPh_3). X-ray Structure of $[(\eta^5\text{-}C_5H_5)Ru(^{i}Pr\text{-}DAB)(\eta^2\text{-propen})[CF_3SO_3]^+$. *Organometallics* **1994**, *13*, 3269−3278. (e) Flsh, R. H.; Klm, H.-S.; Fong, R. H. Bonding Studies of Nltrogen Heterocyclic Ligands to (η^5-Cyclopentadienyl)ruthenium Cation: A Novel Nitrogen to T Rearrangement. *Organometallics* **1989**, *8*, 1375−1377. (f) Fish, R. H.; Kim, H.-S.; Fong, R. H. Bonding Mode of Nitrogen Heterocyclic Ligands to (η^5-Cyclopentadienyl)ruthenium Cation and Reactivity Studies of the Nitrogen and π-Bonded Complexes: Mechanistic Aspects of a Nitrogen to π-Rearrangement. *Organometallics* **1991**, *10*, 770−777. (g) Mbaye, M. D.; Demerseman, B.; Renaud, J.-L.; Toupet, L.; Bruneau, C. $[Cp^*(\eta^2\text{-bipy})(MeCN)Ru^{II}][PF_6]$ Catalysts for Regioselective Allylic Substitution and Characterization of Dicationic $[Cp^*(\eta^2\text{-bipy})\text{-}(\eta^3\text{-allyl})Ru^{IV}][PF_6]_2$ Intermediates. *Angew. Chem., Int. Ed.* **2003**, *42*, 5066−5068.

(3) (a) Bauer, E. B. Chiral-at-metal complexes and their catalytic applications in organic synthesis. *Chem. Soc. Rev.* **2012**, *41*, 3153−3167. (b) Hintermann, L.; Xiao, L.; Labonne, A.; Englert, U. $[CpRu(\eta^6\text{-naphthalene})]PF_6$ as Precursor in Complex Synthesis and Catalysis with the Cyclopentadienyl-Ruthenium(II) Cation. *Organometallics* **2009**, *28*, 5739−5748. (c) Becker, E.; Stingl, V.; Mereiter, K.; Kirchner, K. Formation of a Half-Sandwich Triscarbene Ruthenium Complex: Oxidative Coupling of 2,7-Nonadiyne Mediated by $[RuCp(IPr^{i})(CH_3CN)_2]^+$ (IPri) 1,3-bis(2,6-diisopropylphenyl)-imidazol-2-ylidene). *Organometallics* **2006**, *25*, 4166−4169. (d) Baratta, W.; Herrmann, W. A.; Kratzer, R. M.; Rigo, P. Half-Sandwich Ruthenium(II) Catalysts for C-C Coupling Reactions between Alkenes and Diazo Compounds. *Organometallics* **2000**, *19*, 3664−3669. (e) Baratta, W.; Zotto, A. D.; Rigo, P. Half-Sandwich Ruthenium(II) Complexes as Catalysts for Stereoselective Carbene-Carbene Coupling Reactions. *Organometallics* **1999**, *18*, 5091−5096.

(4) Ashby, G. S.; Bruce, M. I.; Tomkins, I. B.; Wallis, R. C. Cyclopentadienyl-Ruthenium and -Osmium Chemistry. VII* Complexes Containing Nitriles, Tertiary Phosphines or Phosphites Formed by Addition or Displacement Reactions. *Aust. J. Chem.* **1979**, *32*, 1003−1016.

(5) (a) Govindaswamy, P.; Mozharivskyj, Y. A.; Kollipara, M. R. Synthesis and characterization of cyclopentadienylruthenium(II) complexes containing N,N′-donor Schiff base ligands: crystal and molecular structure of $[(\eta^5\text{-}C_5H_5)Ru(C_5H_4N\text{-}2\text{-}CH{=}N{-}C_6H_4{-}p\text{-}OCH_3)(PPh_3)]PF_6$. *Polyhedron* **2004**, *23*, 1567−1572. (b) Pachhunga, K.; Therrien, B.; Kreisel, K. A.; Yap, G. P. A.; Kollipara, M. R. Reactivity studies of cyclopentadienyl ruthenium(II), osmium(II) and pentamethylcyclopentadienyl iridium(III) complexes towards 2-(2′-pyridyl)imidazole derivatives. *Polyhedron* **2007**, *26*, 3638−3644.

(6) (a) Trost, B. M.; Frederiksen, M. U.; Rudd, M. T. Ruthenium-Catalyzed Reactions-A Treasure Trove of Atom-Economic Transformations. *Angew. Chem., Int. Ed.* **2005**, *44*, 6630−6666. (b) Osakada, K. 1,4-Hydrosilylation of Pyridine by Ruthenium Catalyst: A New Reaction and Mechanism. *Angew. Chem., Int. Ed.* **2011**, *50*, 3845−3846.

(7) (a) Mai, V. H.; Kuzmina, L. G.; Churakov, A. V.; Korobkov, I.; Howard, J. A. K.; Nikonov, G. I. NHC carbene supported half-sandwich hydridosilyl complexes of ruthenium: the impact of supporting ligands on Si···H interligand interactions. *Dalton Trans.* **2016**, *45*, 208−215. (b) Clark, J. L.; Duckett, S. B. Photochemical studies of $(\eta^5\text{-}C_5H_5)Ru(PPh_3)_2Cl$ and $(\eta^5\text{-}C_5H_5)Ru(PPh_3)_2Me$: formation of Si-H and C-H bond activation products. *Dalton Trans.* **2014**, *43*, 1162−1171.

(8) Glöge, T.; Jess, K.; Bannenberg, T.; Jones, P. G.; Langenscheidt-Dabringhausen, N.; Salzer, A.; Tamm, M. 16-Electron pentadienyl- and cyclopentadienylruthenium half-sandwich complexes with bis(imidazol-2-imine) ligands and their use in catalytic transfer hydrogenation. *Dalton Trans.* **2015**, *44*, 11717−11724.

(9) (a) Moreno, V.; Font-Bardia, M.; Calvet, T.; Lorenzo, J.; Avilés, F. X.; Garcia, M. H.; Morais, T. S.; Valente, A.; Robalo, M. P. DNA interaction and cytotoxicity studies of new ruthenium(II) cyclopentadienyl derivative complexes containing heteroaromatic ligands. *J. Inorg. Biochem.* **2011**, *105*, 241−249. (b) Tomaz, A. I.; Jakusch, T.; Morais, T. S.; Marques, F.; de Almeida, R. F. M.; Mendes, F.; Enyedy, É. A.; Santos, I.; Pessoa, J. C.; Kiss, T.; Garcia, M. H. $[Ru^{II}(\eta^5\text{-}C_5H_5)(bipy)(PPh_3)]^+$, a promising large spectrum antitumor agent: Cytotoxic activity and interaction with human serum albumin. *J. Inorg. Biochem.* **2012**, *117*, 261−269.

(10) Blum, Y.; Shvo, Y. Catalytically Reactive Ruthenium Intermediates in the Homogeneous Oxidation of Alcohols to Esters. *Isr. J. Chem.* **1984**, *24*, 144−148. (b) Conley, B. L.; Pennington-Boggio, M. K.; Boz, E.; Williams, T. J. Discovery, Applications, and Catalytic Mechanisms of Shvo's Catalyst. *Chem. Rev.* **2010**, *110*, 2294−2312.

(11) Fábos, V.; Mika, L. T.; Horváth, I. T. Selective Conversion of Levulinic and Formic Acids to γ-Valerolactone with the Shvo Catalyst. *Organometallics* **2014**, *33*, 181−187.

(12) Lee, S.-H.; Gutsulyak, D. V.; Nikonov, G. I. Chemo- and Regioselective Catalytic Reduction of N-Heterocycles by Silane. *Organometallics* **2013**, *32*, 4457−4464.

(13) Mai, V. H.; Korobkov, I.; Nikonov, G. I. Half-Sandwich Silane σ-Complexes of Ruthenium Supported by NHC Carbene. *Organometallics* **2016**, *35*, 936−942.

(14) Lee, S.-H.; Nikonov, G. I. Transfer Hydrogenation of Ketones, Nitriles, and Esters Catalyzed by a Half-Sandwich Complex of Ruthenium. *ChemCatChem* **2015**, *7*, 107−113.

(15) Mai, V. H.; Lee, S.-H.; Nikonov, G. I. Transfer Hydrogenation of Unsaturated Substrates by Half-sandwich Ruthenium Catalysts using Ammonium Formate as Reducing Reagent. *Chemistry Select* **2017**, *2*, 7751−7757.

(16) Mai, V. H.; Nikonov, G. I. Transfer Hydrogenation of Nitriles, Olefins, and N-Heterocycles Catalyzed by an N-Heterocyclic Carbene-Supported Half-Sandwich Complex of Ruthenium. *Organometallics* **2016**, *35*, 943−949.

(17) Standfest-Hauser, C.; Slugovc, C.; Mereiter, K.; Schmid, R.; Kirchner, K.; Xiao, L.; Weissensteiner, W. Hydrogen-transfer catalyzed by half-sandwich Ru(II) aminophosphine complexes. *J. Chem. Soc., Dalton Trans.* **2001**, 2989−2995.

(18) Kumar, P.; Singh, A. K.; Sharma, S.; Pandey, D. S. Structures, preparation and catalytic activity of ruthenium cyclopentadienyl complexes based on pyridyl-phosphine ligand. *J. Organomet. Chem.* **2009**, *694*, 3643−3652.

(19) Review on biomass transformations: (a) Corma, A.; Iborra, S.; Velty, A. Chemical Routes for the Transformation of Biomass into Chemicals. *Chem. Rev.* **2007**, *107*, 2411−2502. (b) Morone, A.; Apte, M.; Pandey, R. A. Levulinic acid production from renewable waste resources: Bottlenecks, potential remedies, advancements and applications. *Renewable Sustainable Energy Rev.* **2015**, *51*, 548−565. (c) Serrano-Ruiz, J. C.; Luque, R.; Sepulveda-Escribano, A. Transformations of biomass-derived platform molecules: from high added-value chemicals to fuels *via* aqueous-phase processing. *Chem. Soc. Rev.* **2011**, *40*, 5266−5281. (d) Sankar, M.; Dimitratos, N.; Miedziak, P. J.; Wells, P. P.; Kiely, C. J.; Hutchings, G. J. Designing bimetallic catalysts for a green and sustainable future. *Chem. Soc. Rev.* **2012**, *41*, 8099−8139. (e) Climent, M. J.; Corma, A.; Iborra, S. Conversion of biomass platform molecules into fuel additives and liquid hydrocarbon fuels. *Green Chem.* **2014**, *16*, 516−547. (f) Gupta, K.; Rai, R. K.; Singh, S. K. Metal catalysts for Efficient Transformation of Biomass-derived HMF and Furfural to Value Added Chemicals: Recent Progress. *ChemCatChem* **2018**, DOI: 10.1002/cctc.201701754.

DOI: 10.1021/acs.inorgchem.8b00536
Inorg. Chem. XXXX, XXX, XXX−XXX

(20) Schiavo, V.; Descotes, G.; Montech, J. Catalytic-hydrogenation of 5-hydroxymethyl furfural in aqueous medium. *Bull. Soc. Chim. Fr.* **1991**, *128*, 704−711.
(21) Liu, F.; Audemar, M.; Vigier, K. D. O.; Clacens, J. -M; De Campo, F.; Jérôme, F. Combination of Pd/C and Amberlyst-15 in a single reactor for the acid/hydrogenating catalytic conversion of carbohydrates to 5-hydroxy-2,5-hexanedione. *Green Chem.* **2014**, *16*, 4110−4114.
(22) (a) Hu, X.; Westerhof, R. J. M.; Wu, L.; Dong, D.; Li, C.-Z. Upgrading biomass-derived furans via acid-catalysis/hydrogenation: the remarkable difference between water and methanol as the solvent. *Green Chem.* **2015**, *17*, 219−224. (b) Hu, X.; Song, Y.; Wu, L.; Gholizadeh, M.; Li, C.-Z. One-Pot Synthesis of Levulinic Acid/Ester from C5 Carbohydrates in a Methanol Medium. *ACS Sustainable Chem. Eng.* **2013**, *1*, 1593−1599.
(23) Xu, Z.; Yan, P.; Xu, W.; Liu, X.; Xia, Z.; Chung, B.; Jia, S.; Zhang, Z. C. Hydrogenation/Hydrolytic Ring Opening of 5-HMF by Cp*-Iridium(III)Half-Sandwich Complexes for Bioketones Synthesis. *ACS Catal.* **2015**, *5*, 788−792.
(24) Xu, Z.; Yan, P.; Li, H.; Liu, K.; Liu, X.; Jia, S.; Zhang, Z. C. Active Cp*Iridium(III) Complex with *ortho*-Hydroxyl Group Functionalized Bipyridine Ligand Containing an Electron-Donating Group for the Production of Diketone from 5-HMF. *ACS Catal.* **2016**, *6*, 3784−3788.
(25) Wu, W.-P.; Xu, Y.-J.; Zhu, R.; Cui, M.-S.; Li, X.-L.; Deng, J.; Fu, Y. Selective Conversion of 5-Hydroxymethylfuraldehyde Using Cp*Ir Catalysts in Aqueous Formate Buffer Solution. *ChemSusChem* **2016**, *9*, 1209−1215.
(26) Xu, Y.-J.; Shi, J.; Wu, W.-P.; Zhu, R.; Li, X.-L.; Deng, J.; Fu, Y. Effect of Cp*Iridium(III) Complex and acid co-catalyst on conversion of furfural compounds to cyclopentanones or straight chain ketones. *Appl. Catal., A* **2017**, *543*, 266.
(27) Dwivedi, A. D.; Gupta, K.; Tyagi, D.; Rai, R. K.; Mobin, S. M.; Singh, S. K. Ruthenium and Formic Acid Based Tandem Catalytic Transformation of Bioderived Furans to Levulinic Acid and Diketones in Water. *ChemCatChem* **2015**, *7*, 4050−4058.
(28) Gupta, K.; Tyagi, D.; Dwivedi, A. D.; Mobin, S. M.; Singh, S. K. Catalytic transformation of bio-derived furans to valuable ketoacids and diketones by water-soluble ruthenium catalysts. *Green Chem.* **2015**, *17*, 4618−4627.
(29) Dwivedi, A. D.; Rai, R. K.; Gupta, K.; Singh, S. K. Catalytic Hydrogenation of Arenes in Water Over In Situ Generated Ruthenium Nanoparticles Immobilized on Carbon. *ChemCatChem* **2017**, *9*, 1930−1938.
(30) Dykeman, R. R.; Luska, K. L.; Thibault, M. E.; Jones, M. D.; Schlaf, M.; Khanfar, M.; Taylor, N. J.; Britten, J. F.; Harrington, L. Catalytic deoxygenation of terminal-diols under acidic aqueous conditions by the ruthenium complexes $[(\eta^6\text{-arene})Ru(X)(N\cap N)](OTf)n$, X = H_2O, H, η^6-arene = *p*-Me-^{i}Pr-C_6H_4, C_6Me_6, N∩N= bipy, phen, 6,6′-diamino-bipy, 2,9-diamino-phen, n = 1, 2) Influence of the *ortho*-amine substituent on catalytic activity. *J. Mol. Catal. A: Chem.* **2007**, *277*, 233−251.
(31) Thibault, M. E.; DiMondo, D. V.; Jennings, M.; Abdelnur, P. V.; Eberlin, M. N.; Schlaf, M. Cyclopentadienyl and pentamethylcyclopentadienyl ruthenium complexes as catalysts for the total deoxygenation of 1,2-hexanediol and glycerol. *Green Chem.* **2011**, *13*, 357−366.
(32) DiMondo, D.; Thibault, M. E.; Britten, J.; Schlaf, M. Comparison of the Catalytic Activity of $[(\eta^5\text{-}C_5H_5)Ru(2,2'\text{-bipyridine})(L)]OTf$ versus $[(\eta^5\text{-}C_5H_5)Ru(6,6'\text{-diamino-}2,2'\text{-bipyridine})(L)]OTf$ (L = labile ligand) in the Hydrogenation of Cyclohexanone. Evidence for the Presence of a Metal-Ligand Bifunctional Mechanism under Acidic Conditions. *Organometallics* **2013**, *32*, 6541−6554.
(33) Singh, S. K.; Chandra, M.; Pandey, D. S.; Puerta, M. C.; Valerga, P. Helices of ruthenium complexes involving pyridyl-azine ligands: synthesis, spectral and structural aspects. *J. Organomet. Chem.* **2004**, *689*, 3612−3620.
(34) Bruce, M. I.; Wong, F. S.; Skelton, B. W.; White, A. H. Cyclopentadienyl-ruthenium and -osmium chemistry. Part 11. Reactions and structures of $[RuCl(PPh_3)_2(\eta^5\text{-}C_5H_5)]$ and its trimethyl-phosphine analogue. *J. Chem. Soc., Dalton Trans.* **1981**, 1398−1405.
(35) Becker, E.; Slugovc, C.; Ruba, E.; Standfest-Hauser, C.; Mereiter, K.; Schmidt, R.; Kirschner, K. Synthesis, characterization, and reactivity of half-sandwich Ru(II) complexes containing phosphine, arsine, stibine, and bismutine ligands. *J. Organomet. Chem.* **2002**, *649*, 55−63.
(36) (a) Chakraborty, A. K.; Bischoff, K. B.; Astarita, G.; Damewood, J. R. Molecular orbital approach to substituent effects in amine-CO_2 interactions. *J. Am. Chem. Soc.* **1988**, *110*, 6947−6954. (b) Graton, J.; Berthelot, M.; Laurence, C. Hydrogen-bond basicity pK_{HB} scale of secondary amine. *J. Chem. Soc., Perkin Trans.* **2001**, *2*, 2130−2135.
(37) Lin, Y.-C.; Yu, K.-H.; Huang, S.-L.; Liu, Y.-H.; Wang, Y.; Liu, S.-T.; Chen, J.-T. Alternating ethylene-norbornene copolymerization catalyzed by cationic organopalladium complexes bearing hemilabile bidentate ligands of a-amino-pyridines. *Dalton Trans.* **2009**, 9058−9067.
(38) (a) Tajvidi, K.; Hausoul, P. J. C.; Palkovits, R. Hydrogenolysis of Cellulose over Cu-Based Catalysts-Analysis of the Reaction Network. *ChemSusChem* **2014**, *7*, 1311−1317. (b) Yepez, A.; Garcia, A.; Climent, M. S.; Romero, A. A.; Luque, R. Catalytic conversion of starch into valuable furan derivatives using supported metal nanoparticles on mesoporous aluminosilicate materials. *Catal. Sci. Technol.* **2014**, *4*, 428−434. (c) Alamillo, R.; Crisci, A. J.; Gallo, J. M. R.; Scott, S. L.; Dumesic, J. A. A Tailored Microenvironment for Catalytic Biomass Conversion in Inorganic-Organic Nanoreactors. *Angew. Chem., Int. Ed.* **2013**, *52*, 10349−10351. (d) Zhang, J.; Weitz, E. An in Situ NMR Study of the Mechanism for the Catalytic Conversion of Fructose to 5-Hydroxymethylfurfural and then to Levulinic Acid Using ^{13}C Labeled D-Fructose. *ACS Catal.* **2012**, *2*, 1211−1218. (e) Thananatthanachon, T.; Rauchfuss, T. B. Efficient Route to Hydroxymethylfurans from Sugars via Transfer Hydrogenation. *ChemSusChem* **2010**, *3*, 1139−1141. (f) Nikolla, E.; Roman-Leshkov, Y.; Moliner, M.; Davis, M. E. One-Pot" Synthesis of 5-(Hydroxymethyl)furfural from Carbohydrates using Tin-Beta Zeolite. *ACS Catal.* **2011**, *1*, 408−410.
(39) Crabtree, R. H. Deactivation in Homogeneous Transition Metal Catalysis: Causes, Avoidance, and Cure. *Chem. Rev.* **2015**, *115*, 127−150.

DOI: 10.1021/acs.inorgchem.8b00536
Inorg. Chem. XXXX, XXX, XXX−XXX